

Supplementary data for

Effect of the position of a phenyl group on the luminescent and TNP-sensing properties of cationic iridium(III) complexes

Xiaoran Yang, Jiahao Du, Rui Cai, Chun Liu *

State Key Laboratory of Fine Chemicals, Frontier Science Center for Smart Materials,
School of Chemical Engineering, Dalian University of Technology, Linggong Road 2,
Dalian 116024, China; E-mail: cliu@dlut.edu.cn.

Contents

Materials and instruments *S1*

Synthesis and characterization *S2-S4*

Preparation and Detection of TNP Samples *S4*

Photophysical and AIPE properties *S4*

Detection of TNP *S5*

Sensing Mechanism *S5*

NMR spectra and HRMS of **1**, **2**, and **3** *S6-S10*

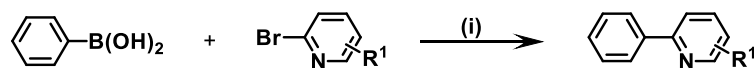
Materials and instruments

All starting materials were purchased from commercial sources and used without further purification. The ¹H NMR spectra were recorded at Bruker AVANCE III 500. The ¹³C NMR spectra was recorded at BRUKER AVANCE NEO 400MHz. Mass spectra were obtained on a Synapt G2-Si HDMS and Agilent G6230B mass spectrometer. Absorption spectra were recorded using Agilent Cary 100 UV-vis spectrophotometer. The emission spectra were recorded with a Hitachi F-7100 fluorescence spectrophotometer. Lifetime decay traces were tested using a transient fluorescence spectrometer FLS1000. The dynamic light scattering (DLS) was measured

on Malvern ZS90.

Synthesis and characterization

Synthesis of ligands L1-L3



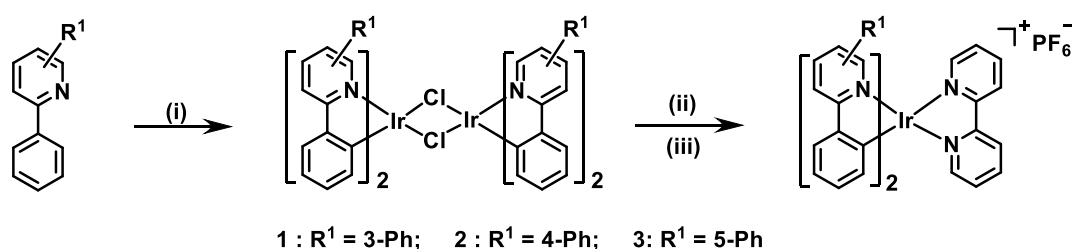
L1 : R¹ = 3-Ph L2 : R¹ = 4-Ph L3 : R¹ = 5-Ph

(i) Pd(OAc)₂, K₂CO₃, EtOH/H₂O 3:1 (v/v), 80 °C air

Figure S1. Synthesis route of the cyclometalating ligands L1-L3.

The cyclometalating ligands were synthesized using the Suzuki-Miyaura reaction catalyzed by Pd(OAc)₂ developed by our group. To a double-necked flask, 0.5 mmol of 2-bromopyridine derivative, phenylboronic acid (3.0 equiv.), potassium carbonate (2.0 equiv.), and palladium acetate (1.5% equiv.) were added sequentially in air, followed by 8 mL of a mixed ethanol-water solution with a volume ratio of 3:1, and the reaction was magnetically stirred for 10-50 min at 80°C. At the end of the reaction, it was extracted with saturated saline and dichloromethane, and the organic phases were combined and concentrated under reduced pressure. The cyclometalating ligands L1-L3 were prepared by column chromatography with petroleum ether/ethyl acetate (30:1) as eluent.

Synthesis and characterization of the complexes 1-3



(i) IrCl₃·3H₂O, EtOCH₂CH₂OH/H₂O, 3:1 (v/v), 120 °C, N₂, 24 h.
(ii) 2,2'-Bipyridine, EtOCH₂CH₂OH, 120 °C, N₂, 24 h. (iii) KPF₆, RT, 3 h.

Figure S2. Synthesis route of the complexes 1-3.

In the first step, IrCl₃·3H₂O (0.20 mmol) was added to a 25 mL double-necked flask, and then cyclometalating ligand (0.5 mmol), 12 mL of a mixed solution of ethylene

glycol monoethyl ether/water in the ratio of 3:1 by volume, was added sequentially, and the reaction was carried out for 24 h at 120°C under nitrogen protection with nitrogen displacement for three times. At the end of the reaction, it was cooled to room temperature and concentrated under reduced pressure to give the intermediate.

In the second step, the above intermediate was transferred to a 50 mL single-necked round-bottomed flask and 2,2'-bipyridine (0.6 mmol) and ethylene glycol monoethyl ether (8 mL) were added. The reaction was carried out under nitrogen atmosphere at 120°C for 24 h. After the reaction, the mixture was cooled to room temperature, and an excess of saturated aqueous solution of KPF₆ (15 equiv.) was added and stirred at room temperature for 3 h. The resulting mixture was extracted with saturated saline and dichloromethane, and the organic phases were combined and concentrated to obtain the crude product. The target product was isolated and purified using dichloromethane as eluent.

1, yellow solid, 130.1 mg, yield: 68%. ¹H NMR (400 MHz, DMSO-*d*₆) δ 8.93 (d, *J* = 8.2 Hz, 2H), 8.31 (t, *J* = 7.8 Hz, 2H), 7.86 (d, *J* = 5.1 Hz, 2H), 7.80 - 7.67 (m, 6H), 7.63 - 7.42 (m, 8H), 7.31 (s, 2H), 7.23 - 7.13 (m, 2H), 6.82 (t, *J* = 7.2 Hz, 2H), 6.66 - 6.52 (m, 4H), 6.30 (d, *J* = 7.5 Hz, 2H). ¹³C NMR (125 MHz, DMSO-*d*₆) δ 163.98, 155.27, 152.27, 149.64, 148.52, 144.12, 141.34, 139.77, 138.91, 136.58, 131.07, 129.55, 129.18, 128.61, 125.19, 123.21, 121.15. HRMS (Synapt G2-Si HDMS, *m/z*): calcd for C₄₄H₃₂N₄Ir [M - PF₆]⁺ 809.2251, found 809.2251.

2, yellow solid, 132.6 mg, Yield: 70%. ¹H NMR (400 MHz, DMSO-*d*₆) δ 8.93 (d, *J* = 8.1 Hz, 2H), 8.59 (d, *J* = 1.2 Hz, 2H), 8.31 (t, *J* = 7.6 Hz, 2H), 8.20 (d, *J* = 7.7 Hz, 2H), 7.98 (dd, *J* = 13.8, 6.1 Hz, 6H), 7.79 - 7.71 (m, 2H), 7.64 (d, *J* = 6.2 Hz, 2H), 7.61 - 7.50 (m, 8H), 7.06 (t, *J* = 7.4 Hz, 2H), 6.96 (t, *J* = 7.2 Hz, 2H), 6.34 (d, *J* = 7.5 Hz, 2H). ¹³C NMR (125 MHz, DMSO-*d*₆) δ 166.47, 155.37, 150.91, 150.06, 149.08, 143.29, 141.41, 140.09, 139.64, 138.81, 128.80, 128.75, 127.54, 126.36, 125.51, 125.00, 123.91, 121.21, 120.23. HRMS (ESI, *m/z*): calcd for C₄₄H₃₂N₄Ir [M - PF₆]⁺ 809.2251, found 809.2255.

3, yellow solid, 171.7 mg, yield: 90%. ¹H NMR (400 MHz, DMSO-*d*₆) δ 8.88 (d, *J* = 8.2 Hz, 2H), 8.39 (d, *J* = 8.6 Hz, 2H), 8.31 (dd, *J* = 12.6, 6.3 Hz, 4H), 8.04 (d, *J* = 5.3 Hz, 2H), 8.00 (d, *J* = 7.7 Hz, 2H), 7.80 - 7.72 (m, 2H), 7.64 (s, 2H), 7.41 (t, *J* = 6.3 Hz, 6H), 7.37 (d, *J* = 7.8 Hz, 4H), 7.06 (t, *J* = 7.5 Hz, 2H), 6.95 (t, *J* = 7.4 Hz, 2H), 6.31 (d, *J* = 7.5 Hz, 2H). ¹³C NMR (125 MHz, DMSO-*d*₆) δ 165.92, 155.70, 150.42, 150.04, 145.36, 143.37, 139.71, 136.88, 135.18, 134.75, 131.02, 130.50, 129.35, 128.88,

128.77, 126.28, 125.36, 122.44, 120.28. HRMS (LTQ Orbitrap XL, m/z): calcd for $C_{44}H_{32}N_4Ir [M - PF_6]^+$ 809.2251, found 809.2251.

Preparation and Detection of TNP Samples

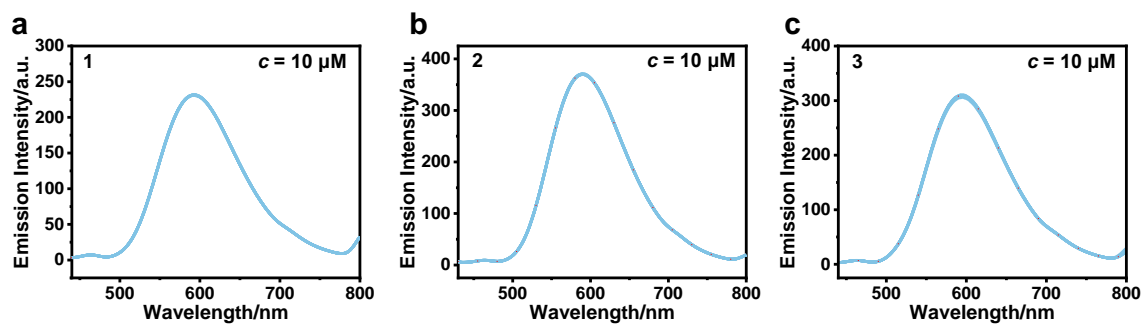


Figure S3. The emission spectra of **1**, **2**, and **3** in 11 blank samples in CH_3CN/H_2O ($f_w = 60\%$, $10 \mu M$).

Photophysical and AIPE properties

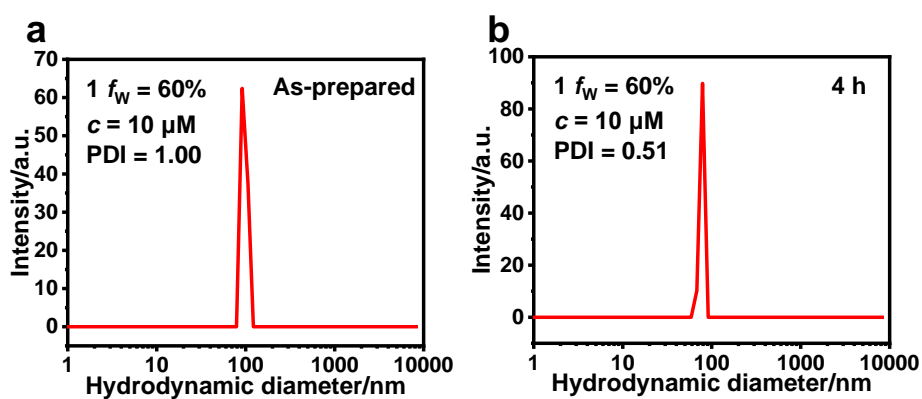


Figure S4. DLS analysis of **1** at 60% water content ($10 \mu M$, CH_3CN/H_2O).

Detection of TNP

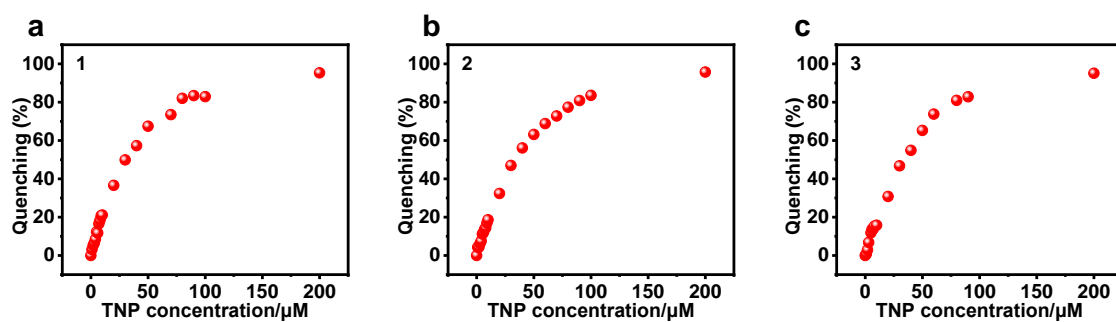


Figure S5. The quenching percentages of **1**, **2**, and **3** after addition of TNP at various concentrations.

Table S1. The emission intensity of **1**, **2**, and **3** at λ_{em} nm in 11 blank samples in CH₃CN/H₂O ($f_w = 60\%$, 10 μ M).

	λ_{em}	X ₁	X ₂	X ₃	X ₄	X ₅	X ₆	X ₇	X ₈	X ₉	X ₁₀	X ₁₁	σ
1	592	231.0	230.8	230.7	231.1	231.2	231.1	231.5	231.3	231.7	231.7	231.5	0.29
2	591	369.3	369.6	369.9	369.8	369.9	369.7	369.6	369.8	369.9	370.2	370.9	0.41
3	594	309.7	310.4	309.0	310.3	309.8	309.2	308.7	308.5	308.9	309.0	309.9	0.65

Sensing Mechanism

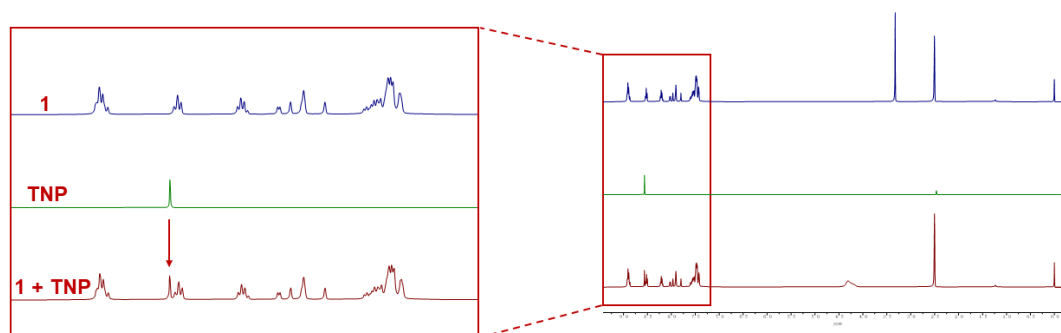


Figure S6. ¹H NMR spectra of **1**, TNP, and **1** + TNP.

NMR spectra and HRMS of 1, 2, and 3

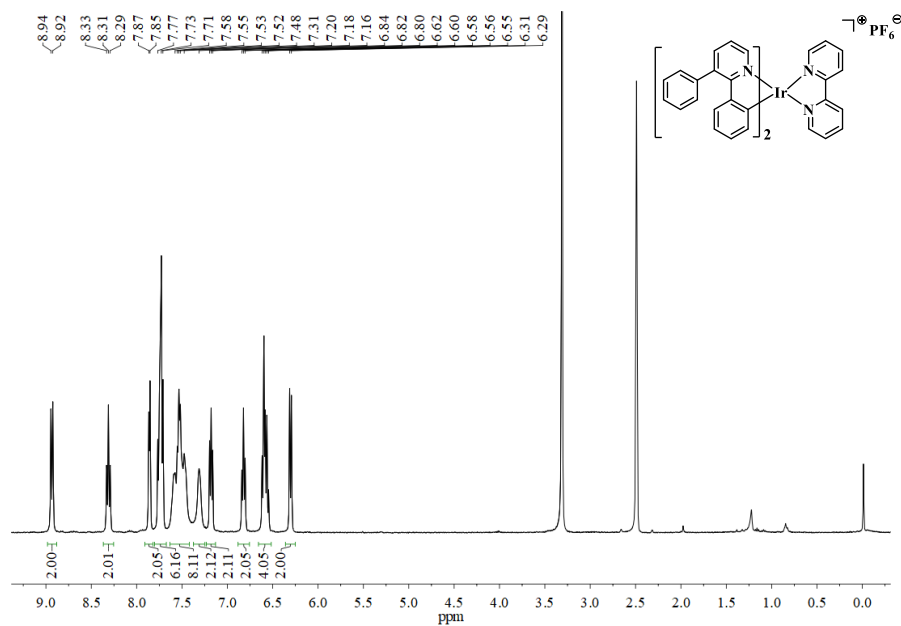


Figure S7. ^1H NMR spectrum of **1** in $\text{DMSO-}d_6$.

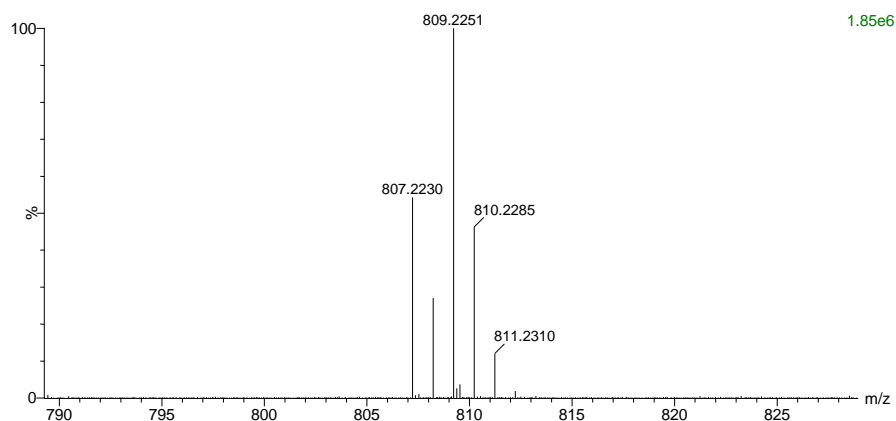


Figure S8. The HRMS of cationic portion of **1**.

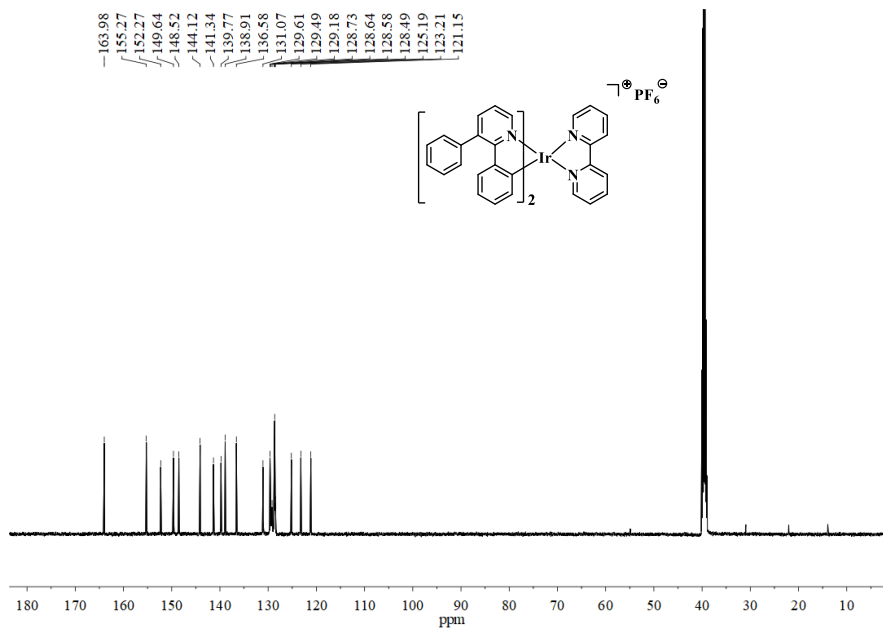


Figure S9. ^{13}C NMR spectrum of **1** in $\text{DMSO-}d_6$.

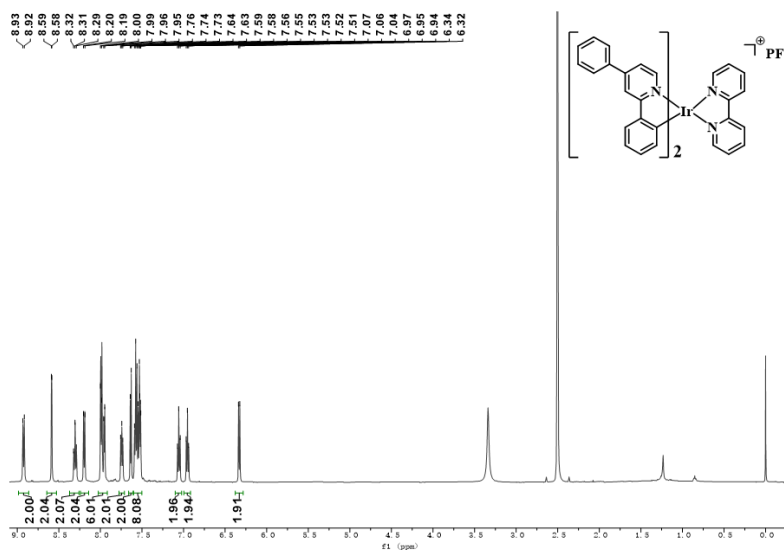


Figure S10. ^1H NMR spectrum of **2** in $\text{DMSO-}d_6$.

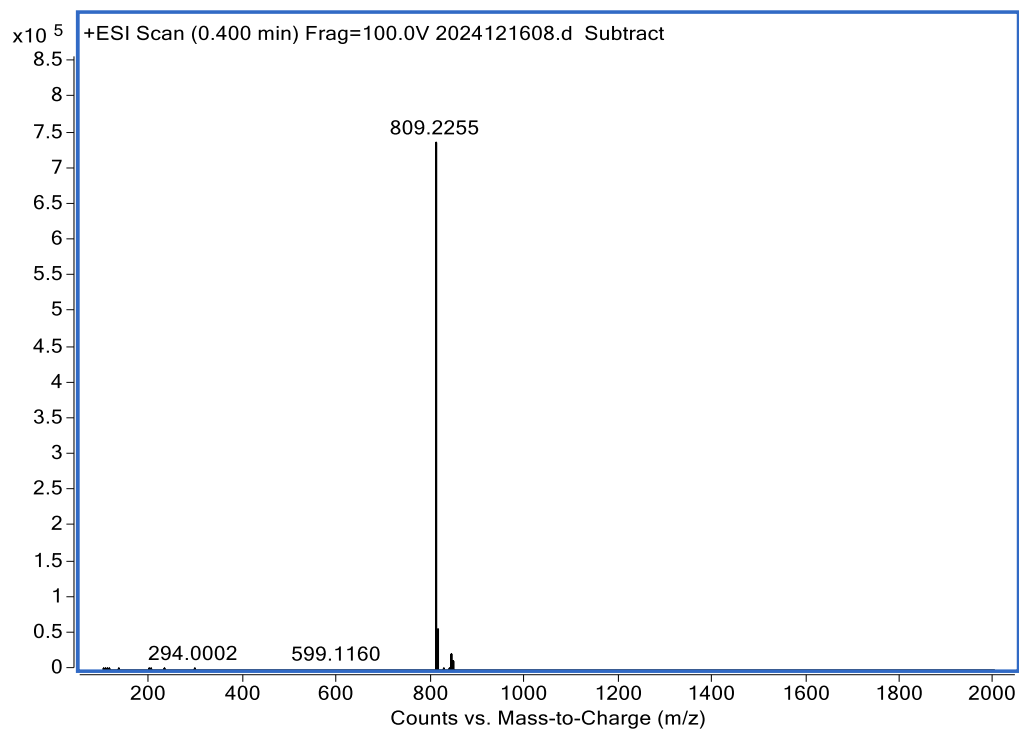


Figure S11. The HRMS of cationic portion of **2**.

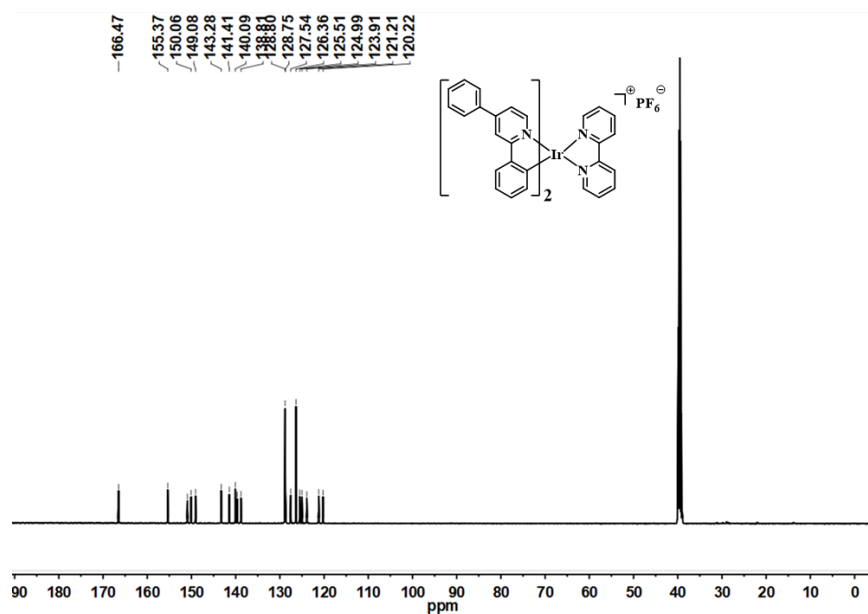


Figure S12. ¹³C NMR spectrum of **2** in DMSO-*d*₆.

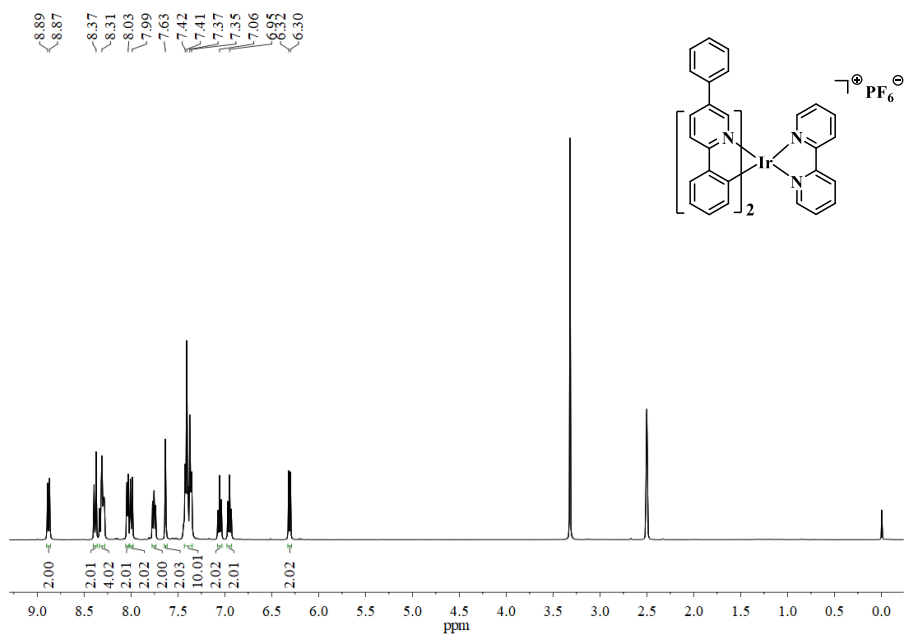


Figure S13. ^1H NMR spectrum of **3** in $\text{DMSO-}d_6$.

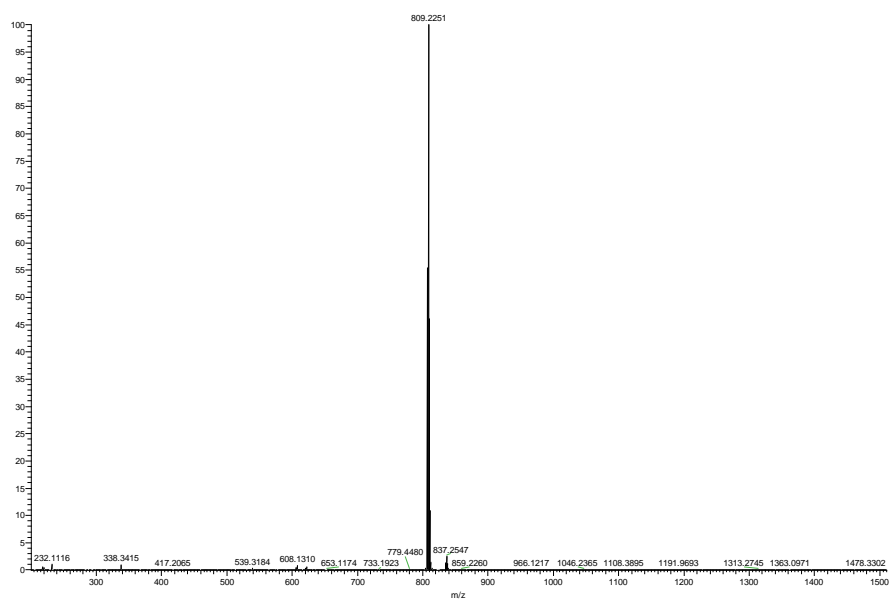


Figure S14. The HRMS of cationic portion of **3**.

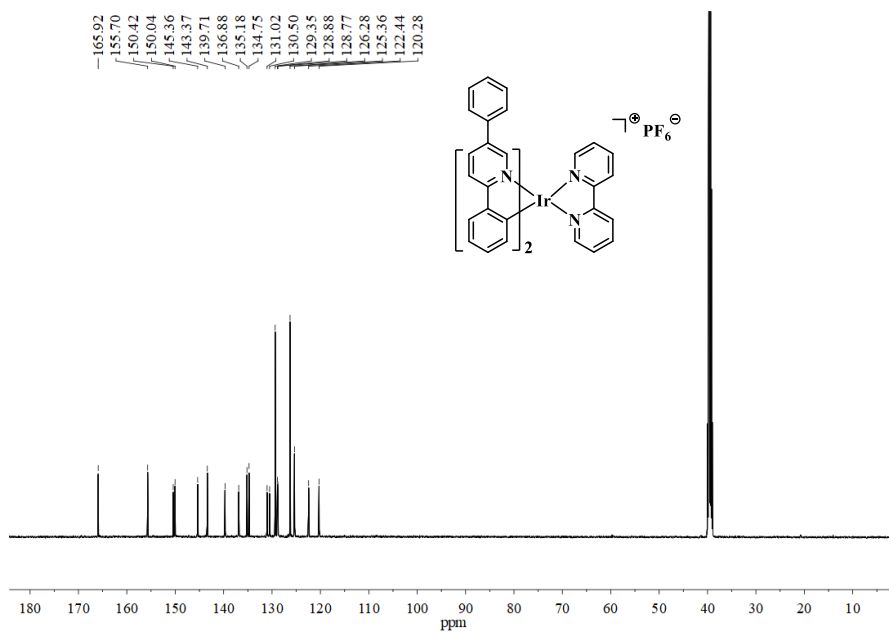


Figure S15. ^{13}C NMR spectrum of **3** in $\text{DMSO-}d_6$.